SIMULATION OF ELECTRICAL

INTERACTION OF CARDIAC CELLS

DENNIS B. HEPPNER *and* ROBERT PLONSEY

From the Biomedical Engineering Department, Case Western Reserve University, Cleveland, Ohio 44106. Dr. Heppner's present address is the Life Sciences Section, Convair Division, General Dynamics Corporation, San Diego, California 92112.

ABSTRACT   A model of the electrical activity of excitable membrane was used to simulate action potential propagation in cardiac cells. Using an implicit method for solving finite difference equations, propagation through the intercalated disc region between two abutting cells was studied. A model of interaction was constructed and parameters of the cellular junction determined. Estimates of the intercalated disc resistance were then made from these junction parameters using a field analysis of the junction. Values of approximately 4 Ω-cm^2 were found and correlate well with experimentally measured values.

INTRODUCTION

The spread of electrical activity in the heart has long been observed to resemble the propagation phenomena observable in a single cell. This behavior is responsible for the characterization of the heart as a functional syncytium. However, anatomically, the heart is known to consist of many cells, each bounded by a plasma membrane and separated from each other by an intercalated disc. The question arises, therefore, whether activity spreads by local circuit current (as would be true in a single axon) or by some other mechanism.

Electrical transmission between cells requires a sufficiently low membrane resistance so that a transthreshold local circuit current can build up in inactive cells adjoining an active one. From a model of end-to-end interaction of cardiac cells, Woodbury and Crill (1), utilizing a simplified analysis, determined that the disc resistance must not exceed 1–5 Ω-cm^2 for electrical transmission to take place. This paper utilizes a similar model but considers the problem in a more rigorous way. Specifically, except for the disc, all membrane is assumed excitable and described by the Hodgkin-Huxley equations as modified by Noble (2). Furthermore, the gap is treated by a rigorous field-theoretic analysis. While the results, in general, agree with those of Woodbury and Crill (1), the limitations and implications of the analysis are established. Furthermore, the same technique utilized in this paper can be applied to the analysis of the finite (terminated) axon.

This paper, subject to stated approximations, describes the electrical properties that the intercalated disc must have if propagation is to occur as a result of local circuit current. That the disc does indeed have such characteristics is not under consideration in this paper. Results presented here neither confirm nor deny the prevalent view that the spread of activity in the heart is electrical in nature (3–5).

MATHEMATICAL TREATMENT OF INTERACTION MODEL

The model considered is sketched in Fig. 1, and illustrates the end-to-end abutment of two cardiac cells. Each cell is assumed cylindrical with a diameter of 15 μ and length 100 μ. The two adjoining end faces constitute the intercalated disc and are assumed inexcitable. The gap region is assumed contiguous with the interstitial media and has the same specific conductivity. All remaining membrane is described by the Hodgkin-Huxley equations as modified by Noble.

Even the (presumably) low resistance disc membrane can be expected to have a high specific resistivity compared to the axoplasm or gap (this will be checked later). Therefore, the assumption is made that the current is orthogonal to the end caps and, in addition, that the axoplasmic surface adjoining the disc is essentially an equipotential. As a consequence, the current field in the membrane is uniform and the membrane thickness is not pertinent; we consider it to be infinitesimal and, hence, describable as a surface discontinuity.

The fields in the gap can be evaluated in terms of the parameters in the above model, based on the aforementioned assumptions. From this solution, a passive network representation of the gap and disc can be formulated. This is necessary in order to electrically represent the coupling of an active and inactive cell; the final goal is a core conductor model of both cardiac cells and the intercalated disc gap region which separates them.

Field Theoretic Analysis of the Gap Region

This section deals with the rigorous solution of the potential field in the intergap region between the two cells shown in Fig. 1. Two identical, cylindrical fibers of radius r_o are abutted together with separation δ. Cylindrical coordinates are chosen as indicated. One fiber is assumed active, the other inactive. The potential field
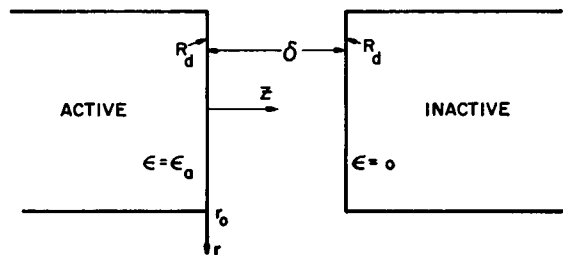

FIGURE 1 Model of cardiac cell interaction—the intercalated disc.

$\epsilon(r, z)$ is desired in the region, $0 < z < \delta; 0 \le r \le r_o$. It is assumed that each fiber is capped with a membrane that is nonexcitable and characterized by a specific resistance $R_d(\Omega\text{-cm}^2)$.

The following analysis will be valid under the assumption that the end-cap resistances R_d are completely passive and independent of voltage and that the current flow depends only on the voltage drop across the gap. The potential of the inactive cell is taken to be zero since the cell is at rest. The potential assigned to the active cell will be a constant ϵ_a, relative to the resting potential. Therefore, determination of R_d under "electrotonic" conditions will give values that are assumed to remain constant under active conditions. In the region of interest, ϵ will satisfy Laplace's equation $\nabla^2\epsilon(r, z) = 0$ which in cylindrical coordinates, with no θ variation due to symmetry, becomes

$$\frac{1}{r} \frac{\partial}{\partial r} \left(r \frac{\partial \epsilon}{\partial r} \right) + \frac{\partial^2 \epsilon}{\partial z^2} = 0. \tag{1}$$

Boundary conditions are considered in terms of the normal current density at the surfaces $z = 0$ and $z = \delta$ and the behavior of ϵ at $r = 0$ and $r = r_o$. These are:

$$(a) \ \frac{\epsilon(r, 0^+) - \epsilon_a}{R_d} = \sigma \left. \frac{\partial \epsilon}{\partial z} \right|_{z=0^+},$$

$$(b) \ \frac{\epsilon(r, \delta^-)}{R_d} = -\sigma \left. \frac{\partial \epsilon}{\partial z} \right|_{z=\delta^-},$$

$$(c) \ \epsilon \text{ finite at } r = 0,$$

$$(d) \ \epsilon = 0 \text{ at } r = r_o.$$

The above relations assume that the membranes are very thin and are located at $z = 0$ and $z = \delta$. The solution to equation 1 is then to be found in the open interval $(0, \delta)$. Conditions (a) and (b) equate the current density crossing each disc membrane to the normal derivative of the field at the interface times the conductivity σ of the medium. Condition (d) is the condition that the external medium be the reference. It must be kept in mind that δ will be very small (order r_o per 1000) and, therefore, the potential in the gap need not be the same as in the external medium even though the two are contiguous.

Solution of equation 1 requires Bessel functions of the first kind in r and hyperbolic functions in z. Conditions (c) and (d) impose a solution in the form

$$\epsilon(r, z) = \sum_{n=1}^{\infty} J_0(k_n r)[A_n \cosh (k_n z) + B_n \sinh (k_n z)], \tag{2}$$

where k_n are the roots of $J_0(k_n r_o) = 0$. Applying boundary conditions (a) and (b) gives

$$\sum_{n=1}^{\infty} A_n J_0(k_n r) - \epsilon_a = R_d \sum_{n=1}^{\infty} k_n B_n J_0(k_n r),$$

and

$$\sum_{n=1}^{\infty} J_0(k_n r)[A_n \cosh (k_n\delta) + B_n \sinh (k_n\delta)]$$

$$= R_d\sigma \sum_{n=1}^{\infty} J_0(k_n r)k_n[A_n \sinh (k_n\delta) + B_n \cosh (k_n\delta)].$$

Multiplying both sides of the above two equations by $rJ_0(k_m r)$, integrating with respect to r over $[0, r_o]$, and using the orthogonality property of the Bessel functions, permit one to solve for A_n and B_n. The final solution is found by substituting the resulting expressions into equation 2 and this yields

$$\frac{\epsilon(r, z)}{\epsilon_a} = \sum_{n=1}^{\infty} \frac{2J_0(k_n r)}{(d_n + \sigma R_d k_n)k_n r_o J_1(k_n r_o)} \cdot [d_n \cosh (k_n z) - \sinh (k_n z)], \quad (3)$$

where

$$d_n = [\sigma R_d k_n + \tanh (k_n\delta)]/[1 + \sigma R_d k_n \tanh (k_n\delta)].$$

The above equation was evaluated for the following set of conditions where the geometrical data are considered to be "typical":

$$r_o = 8 \ \mu,$$

$$\delta = r_o/10^3 = 80 \ A,$$

$$\sigma = 0.02 \ mho/cm,$$

$$R_d \ in \ the \ range \ 0.1–100.0 \ \Omega\text{-}cm^2.$$

The series was arbitrarily terminated at $n = 16$, the terms thereafter adding negligibly to the sum. The results are shown in Fig. 2 with the disc resistance as a param-
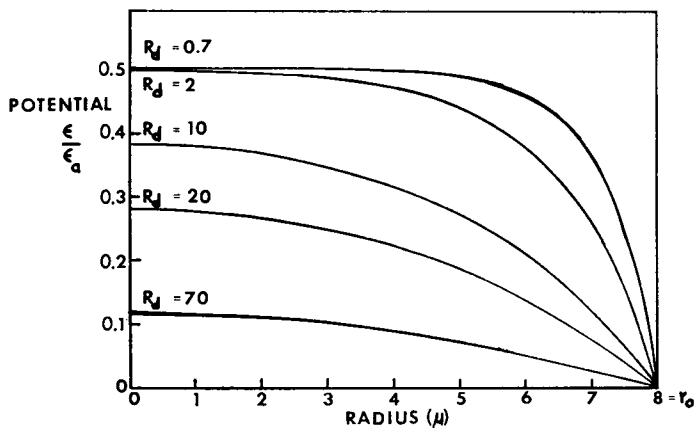

FIGURE 2 Calculated potential field in gap region—evaluated at $z = \delta/2$, R_d, disc resistance, in Ω-cm².

eter. This set of curves was evaluated for $z = \delta/2$ but examination of equation 3 shows that the dependence of ϵ upon z is very slight. This is due to $k_n z$ (for $0 \leq z \leq \delta$) being very small. For instance, if $k_0 r_0 = 2.4$, then $k_0 \delta = 0.0024$. For nearly all values of n and z, therefore, $\cosh (k_n z) \sim 1.0$ and $\sinh (k_n z) \sim 0.0$. Physically this means that at any r value, the intercellular potential drop occurs mainly across the disc resistances with relatively little change in potential across the gap. This is not surprising since the gap has a much higher conductance than the disc. Nevertheless, the field analysis must take into account a z-variation of potential in equation 1 even though it be very small since it is necessary for a correct evaluation of normal current density, which is not negligible.

Woodbury and Crill (1), using the same geometry and boundary conditions, obtained the following differential equation from an elemental-volume treatment of the gap region (where the z-variation in potential is neglected):

$$\frac{d\epsilon}{dr} = \frac{-r}{\lambda^2} (\epsilon_a - 2\epsilon).$$

The solution to this equation, subject to the boundary conditions stated previously, is

$$\frac{\epsilon(r)}{\epsilon_a} = \frac{1}{2}\left[1 - \exp\left(\frac{-r_0^2}{\lambda^2} + \frac{r^2}{\lambda^2}\right)\right], \qquad (4)$$

where $\lambda^2 = 2\delta\sigma R_d$. This expression has been subsequently revised by Woodbury and Crill (6). The new solution appears as equation 5 in the following paper and a plot of it and the above equation 4 are shown in Woodbury and Crill's Fig. 1 B. Woodbury and Crill's original interpretation of their curves is that effective transmission can occur only for R_d less than about 2 Ω-cm^2. This is because for this condition most of the current crossing the active cell surface continues into the inactive cell. However, the question is not only how the current divides between longituinal and radial components in the gap, but what the actual quantities are and how these relate to the attainment of threshold conditions in the inactive cell. It is these questions which are answered in the following treatment.

Current Calculations in the Gap Region

The current density in the gap region is equal to $-\sigma\nabla\epsilon$ where ϵ is given by equation 3. In order to obtain a passive electrical representation of the gap, the current crossing the three surfaces which bound the gap will now be evaluated. These consist of the currents crossing the active and inactive disc surfaces and that crossing the cylindrical wall at $r = r_o(0 < z < \delta)$. We designate these currents as I_1, I_3, and I_2 respectively. The total current entering the gap from the active cell, I_1, is found by computing the density $-\sigma\partial\epsilon/\partial z$ at the surface $z = 0$, multiplying by an elemental

area $2\pi r\, dr$ and integrating over the circular cap surface. Thus

$$I_1 = -2\pi\sigma \int_0^{r_o} r \frac{\partial\epsilon}{\partial z}\bigg|_{z=0} dr.$$

Likewise, the current into the inactive cell is

$$I_3 = -2\pi\sigma \int_0^{r_o} r \frac{\partial\epsilon}{\partial z}\bigg|_{z=\delta} dr.$$

In a similar way the net current, I_2, across the cylindrical gap boundary $(r = r_o, 0 < z < \delta)$ is:

$$I_2 = -2\pi r_o \sigma \int_0^\delta \frac{\partial\epsilon}{\partial r}\bigg|_{r=r_o} dz.$$

Now if equation 3 is substituted into the above three equations and the order of summation and integration interchanged, the following result is achieved after suitable rearrangement,

$$I_1 = 4\pi\sigma r_o \epsilon_a \sum_{n=1}^\infty \frac{1}{c_n}, \tag{5}$$

$$I_3 = -4\pi\sigma r_o \epsilon_a \sum_{n=1}^\infty \frac{1}{c_n} [d_n \sinh(k_n\delta) - \cosh(k_n\delta)], \tag{6}$$

$$I_2 = 4\pi\sigma r_o \epsilon_a \sum_{n=1}^\infty \frac{1}{c_n} [d_n \sinh(k_n\delta) - \cosh(k_n\delta) + 1], \tag{7}$$

where

$$c_n = (d_n + \sigma R_d k_n) k_n r_o,$$

$$d_n = \frac{\sigma R_d k_n + \tanh(k_n\delta)}{1 + \sigma R_d k_n + \tanh(k_n\delta)}.$$

It is apparent from equations 5–7 that $I_2 + I_3 = I_1$ as is required from continuity considerations.

Using the same range of R_d, as previously stated, these currents were computed and are plotted in Fig. 3. The values of current are nondimensional and must be multiplied by the factor $4\pi\sigma r_o \epsilon_a$ to get actual values. It is seen that while the relative quantity I_2/I_1 increases as R_d increases, the actual quantity I_2 decreases since the total amount, I_1, diminishes. Conversely, as R_d decreases, more current enters from the active cell and also more is diverted to the inactive cell. Both of these factors make excitation of the inactive cell more likely at the lower ranges of R_d.

Resistance Calculations of the Gap Region

In this section we shall develop a resistance network to represent the effect of the gap region in splitting the current I_1 into a longitudinal (I_3) and radial (I_2) compo-
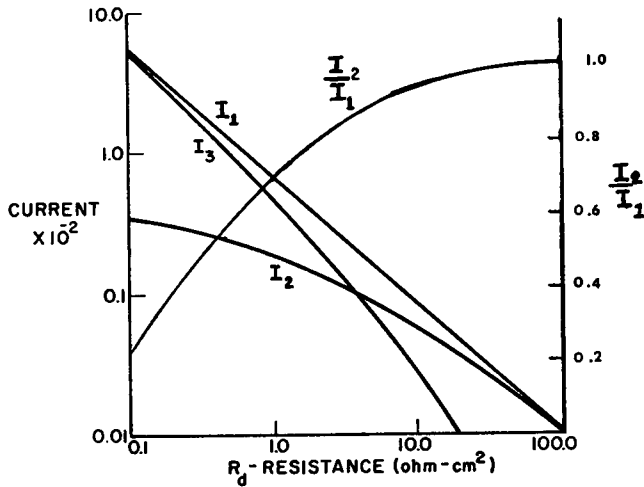
FIGURE 3

FIGURE 4

FIGURE 3 Gap currents I_1, I_2, I_3, and I_2/I_1 vs. R_d.
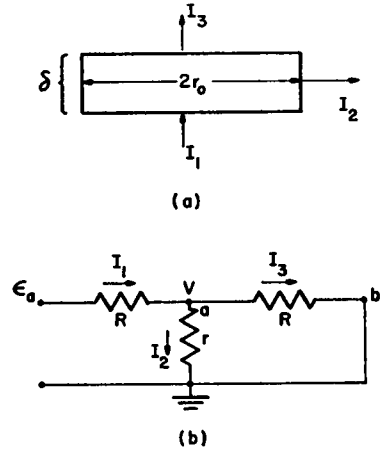
FIGURE 4 Pillbox and simple network representation of gap.

nent. This will be used to couple distributed parameter models of the two adjoining cells so that their interaction can be studied.

Fig. 4 *b* is a simplified network representation of the gap region as described in Fig. 4 *a*. R represents the effective cap (intercalated disc) resistance of each adjoining fiber, while r is an equivalent resistance between the intragap region and the external medium and accounts for transverse current flow. The currents I_1, I_2, and I_3 are those which flow in the corresponding resistances R, r, and R; the network is seen to assign longitudinal current to I_1 and I_3 while transverse current is represented by I_2. ϵ_a is the applied voltage relative to the resting value. The voltage at point b is taken to be zero since the inactive cell is assumed to be at resting conditions, and in this simple model the potential at any point is chosen as the deviation from the resting value, an assumption made in the derivation of equation 3.

Relations for R and r are easily determined by elementary circuit analysis.

$$R = \frac{\epsilon_a}{2I_1 - I_2}, \qquad (8\ a)$$

$$r = \frac{(I_1 - I_2)\epsilon_a}{2I_1 I_2 - I_2^2}. \qquad (8\ b)$$

Various sets of values for R and r were calculated following substitution of equations 5 and 7 for I_1 and I_2, respectively. Notice that the final expressions are independent of the constant ϵ_a. Results for $r_o = 8\ \mu$ and $\delta = r_o/10^2$, $r_o/10^3$, are shown in Table I where R_d is the independent variable. These will be used to estimate values

COMPUTED VALUES OF GAP RESISTANCES R AND r AS A
FUNCTION OF R_d (IN Ω-cm^2).

Entries given for two values of cell separation, δ.

R^a	$\delta = r_o/10^2$		$\delta = r_o/10^3$	
	R	r	R	r
	Ω	Ω	Ω	Ω
0.1	5.1×10^4	1.3×10^5	5.1×10^4	5.1×10^5
0.2	1.0×10^5	1.7	1.0×10^5	6.2
0.3	1.5	1.9	1.5	7.1
0.4	2.0	2.0	2.0	7.8
0.5	2.6	2.2	2.6	8.4
0.7	3.6	2.3	3.6	9.6
1.0	5.1	2.5	5.1	1.1×10^6
2.0	1.0×10^6	2.8	1.0×10^6	1.4
4.0	2.0	3.0	2.0	1.7
5.0	2.6	3.0	2.6	1.8
7.0	3.6	3.10	3.6	1.9
10.0	5.1	3.14	5.1	2.1
20.0	1.0×10^7	3.18	1.0×10^7	2.3
40.0	2.0	3.18	2.0	2.40
50.0	2.6	3.17	2.6	2.47
60.0	3.1	3.16	3.1	2.49
70.0	3.6	3.17	3.6	2.50
100.0	5.1	3.17	5.1	2.53

of R_d that allow intercellular transmission. This is accomplished by first finding values of R and r that permit interaction and then consulting Table I for a determination of the corresponding R_d.

It is interesting to note that the values of R, calculated using equation 8 a, correspond quite closely to those found by dividing R_d by the cross-sectional area, πr_o^2.[1] This conforms to the assumption, expressed earlier, that the field in the intercalated disc is normal to the surface and to the observation that it accounts for most of the drop in potential between the two cells.

CORE CONDUCTOR MODEL OF CARDIAC FIBER INCLUDING GAP

This study uses the core conductor model of the nerve as the basis for examining the dynamic interaction of two fibers. Fig. 5 is the electrical network representation of a short section, Δx, of the core conductor model. The entire fiber consists of an itera-

---

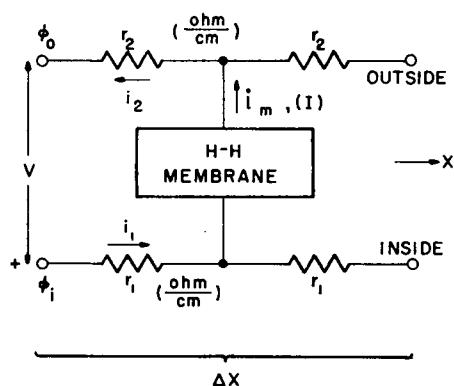[1] See the following paper for a derivation of this simplification employing the closed form solution for the potential.

FIGURE 5 Core conductor model of membrane—section length Δx.

tive structure of this elemental configuration. The intracellular and extracellular media are taken to be passive volume conductors of longitudinal resistances (per unit length) r_1 and r_2, respectively. The longitudinal currents associated with these resistances are i_1 and i_2. The internal and external potentials are denoted Φ_i and Φ_o, and the transmembrane voltage V equals $\Phi_i - \Phi_o$. The membrane is represented by the parallel box labelled "H-H membrane," referring to the Hodgkin-Huxley relationship between the transmembrane current per unit length (i_m) or current per unit area (I) and the transmembrane voltage, V.

The Hodgkin-Huxley membrane model (7, 8) as modified by Noble (9) for application to cardiac cells, formulates the transmembrane current I as

$$I = C\frac{\partial V}{\partial t} + (g_{k_1} + g_{k_2})(V - V_k) + g_{Na}(V - V_{Na}), \qquad (9)$$

where

$$g_{k_1} = 0.0012 \exp[(-V + V_r)/50] + 1.5 \times 10^{-5} \exp[(V + V_r)/60], \quad (10)$$

$$g_{k_2} = \bar{g}_{k_2} n^4, \qquad (11)$$

$$g_{Na} = \bar{g}_{Na} m^3 h + 1.4 \times 10^{-4}, \qquad (12)$$

and V_k, V_{Na} are the potassium and sodium Nernst potentials while V_r is the resting potential. All voltage and current variables are functions of x and t. The n, m, and h parameters are found from three first-order equations of the form

$$\frac{\partial y}{\partial t} = -(\alpha_y + \beta_y)y + \alpha_y, \qquad (13)$$

where $y = n, m,$ or h and

$$\alpha_n = \frac{0.0001(-V + V_r + 40)}{\exp\left[(-V + V_r + 40)/10\right] - 1},$$

$$\beta_n = 0.00125 \exp\left[(-V + V_r)/80\right],$$

$$\alpha_m = \frac{0.1(-V + V_r + 42)}{\exp\left[(-V + V_r + 42)/15\right] - 1},$$

$$\beta_m = \frac{0.12(V + V_r + 98)}{\exp\left[(V + V_r + 98)/5\right] - 1},$$

$$\alpha_h = 0.07 \exp\left[(-V + V_r)/20\right],$$

$$\beta_h = \frac{1.0}{\exp\left[(-V + V_r + 48)/10\right] + 1}. \quad (14)$$

After relating the transmembrane voltage and the longitudinal current of equation 9, one obtains the following expression,

$$\frac{\partial^2 V}{\partial x^2} = 2\pi a(r_1 + r_2)\left[C\frac{\partial V}{\partial t} + (g_{k_1} + g_{k_2})(V - V_k) + g_{\mathrm{Na}}(V - V_{\mathrm{Na}})\right]. \quad (15)$$

Solution of the above equation gives the transmembrane voltage at all points along the fiber and for all time subject to the proper initial and boundary conditions.
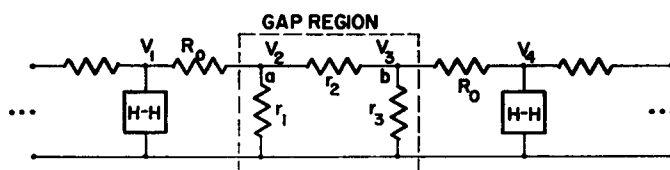

FIGURE 6   Model of cell interaction.

Implementation of an interaction model first assumes that we have two fibers in end-to-end abutment. The network shown in Fig. 4 with resistances R and r will be assumed to approximate the passive electrical behavior of the gap. Instead of this T-type network, it is convenient to let the gap be represented as a π-type equivalent network. The relationships between the T- and π-type parameters are:

$$r_1 = r_3 = 2r + R, \quad (16)$$

$$r_2 = \frac{R}{r}(2r + R). \quad (17)$$

The distributed parameter model of the interaction system is shown in Fig. 6. In order to couple the two cells, two nodes are designated a and b, as illustrated in Fig. 6. If V_1, V_2, V_3, and V_4 are the voltages at the nodes shown, current summation at a and b gives

$$\frac{V_1 - V_2}{R_o} = \frac{V_2}{r_1} + \frac{V_2 - V_3}{r_2}, \quad (18)$$

and

$$\frac{V_2 - V_3}{r_2} = \frac{V_3}{r_3} + \frac{V_3 - V_4}{R_o}, \tag{19}$$

where R_o is the resistance of the internal medium per unit length. To be consistent with previous notation, the V's in the above equations should be replaced by the algebraically absolute voltages less the resting value. Doing this and introducing equations 16 and 17 into the above two expressions and simplifying, yields the following results.

$$R_A V_1 - R_B V_2 + R_o V_3 = V_r (R_A - R_B + R_o), \tag{20}$$

$$R_o V_2 - R_B V_3 + R_A V_4 = V_r (R_A - R_B + R_o), \tag{21}$$

with

$$R_A = \frac{R}{r}(2r + R),$$

$$R_B = \frac{R}{r}(2r + R) + R_o\left(1 + \frac{R}{r}\right).$$

These two equations provide the necessary coupling between the two fibers and show a dependence on R and r, parameters which characterize the gap's electrical properties. Simultaneous solution of these equations and equation 15 will give the transmembrane voltage at any point along the two fibers.

NUMERICAL SOLUTION OF DYNAMIC EQUATIONS

Equations 15, 20, and 21 characterize the potential at all points along the two fibers, including the gap region, and for all time. For fibers of lengths L_1 and L_2, these equations will be solved in the region $0 \leq x \leq L_1 + L_2$ where $x = 0$ has been chosen arbitrarily to be the left end of the first fiber and $x = L_1 + L_2$ at the right end of the second. At $x = L_1$, the appropriate relations of equations 21 and 22 apply. It will be assumed that propagation proceeds from left to right and that at $t = 0$ the transmembrane voltage is specified. The initial value problem which has been formulated is best handled using difference equation techniques. However, one must be careful in choosing a proper method in order to avoid problems of stability, convergence, and the like. Explicit methods, for example, lead to essentially recursive relations and are strongly dependent on the variable increments for stability and convergence. Implicit methods of solution were chosen since stability can be guaranteed and because they are particularly suitable to problems where the domain of one of the variables is finite. This technique, attributed to Crank and Nicholson (10), will lead to a system of equations to be solved simultaneously.

The basic difference between the implicit and explicit methods arises in the ap-

proximations made for the derivatives in equation 15. Both approximate $\partial^2 V/\partial x^2$ as a second central difference. But whereas explicit methods use a forward difference, the implicit method uses a backward difference in approximating $\partial V/\partial t$. The approximations for the partial derivatives are then substituted into equation 15 with all variables being evaluated at $t + \Delta t$. After rearranging, this becomes,

$$V(x - \Delta x, t + \Delta t) - (2 + \alpha + \beta)V(x, t + t\Delta t) + V(x + \Delta x, t + \Delta t)$$
$$= -\alpha V(x, t) + \gamma, \quad (22)$$

where

$$\alpha = 2\pi a(r_1 + r_2)\, C\, \frac{\Delta x^2}{\Delta t},$$

$$\beta = 2\pi a(r_1 + r_2)\Delta x^2[g_{Na} + g_{k_1} + g_{k_2}],$$

$$\gamma = 2\pi a(r_1 + r_2)\Delta x^2[g_{Na} V_{Na} + (g_{k_1} + g_{k_2})V_K],$$

with g_{Na}, g_{k_1}, and g_{k_2} being evaluated at $(x, t + \Delta t)$ also. While α is a constant, note that β and γ are functions of x and t.

This equation clearly illustrates the implicit method. Since the voltage is known at time t, the left-hand side of equation 22 gives the solutions at three values of x. Alternatively, explicit methods provide for simply a linear combination of the three values at time t.

Equation 22 is the discretized version of equation 15. As such, its solution will give values of the transmembrane voltage at points Δx and Δt apart. The discrete solution will approximate the unknown continuous solution if the discrete solution converges for Δx, $\Delta t \to 0$.

In setting up the solution, the left fiber is subdivided into N subintervals and the right one into M, where N and M are chosen such that the increments are of equal size, i.e., $\Delta x = L_1/N = L_2/M$. The endpoints of the active fiber then are x_0 corresponding to $x = 0$ and x_N corresponding to $x = L_1$, while corresponding points of the inactive fiber are x_{N+1} and x_{N+M}. Equation 22 can then be written as,

$$V(x_{i-1}, t + \Delta t) - (2 + \alpha + \beta_i)V(x_i, t + \Delta t) + V(x_{i+1}, t + \Delta t)$$
$$= -\alpha V(x_i, t) + \gamma_i$$
$$i = 1, \cdots, N - 1, N + 2, \cdots, N + M - 1. \quad (23)$$

For the gap region, equations 20 and 21 apply and can be written in terms of the appropriate subscripts as,

$$R_A V_{N-1} - R_B V_N + R_o V_{N+1} = V_r(R_A + R_B - R_o),$$
$$R_o V_N - R_B V_{N+1} + R_A V_{N+2} = V_r(R_A + R_B - R_o),$$

where the Nth node is the last one of the active fiber and the $N + 1^{st}$ node is the first one of the inactive fiber. Since equation 23 represents a system of linear equations in the unknowns $V(x_i, t + \Delta t)$, it, along with the above two equations, can be written in the following tri-diagonal matrix form having $N + M - 1$ unknowns.

$$
\begin{bmatrix}
-(2 + \alpha + \beta_1) & 1 & & & \\
\cdot & & \cdot & & \cdot \\
 & \cdot & & \cdot & & \cdot \\
 & & R_A & -R_B & R_o \\
 & & & R_o & -R_B & R_A \\
 & & & & \cdot & & \cdot & & \cdot \\
 & & & & & \cdot & & \cdot & & \cdot \\
 & & & & & & \cdot & & \cdot & & \cdot \\
 & & & & & & 1 & -(2 + \alpha + \beta_{N+M-1})
\end{bmatrix}
\times
\begin{bmatrix}
V(x_1, t + \Delta t) \\
\cdot \\
\cdot \\
\cdot \\
V(x_N, t + \Delta t) \\
V(x_{N+1}, t + \Delta t) \\
\cdot \\
\cdot \\
\cdot \\
V(x_{N+M-1}, t + \Delta t)
\end{bmatrix}
$$

$$
=
\begin{bmatrix}
-\alpha V(x_1, t) + \gamma_1 - V(x_o, t + \Delta t) \\
\cdot \\
\cdot \\
\cdot \\
V_r(R_A + R_B - R_o) \\
V_r(R_A + R_B - R_o) \\
\cdot \\
\cdot \\
\cdot \\
-\alpha V(x_{N+M-1}) + \gamma_{N+M-1} \\
-V(x_{N+M}, t + \Delta t)
\end{bmatrix}
\quad (24)
$$

with

$$
R_A = \frac{R}{r}(2r + R); \quad R_B = \frac{R}{r}(2r + R) + R_o\left(1 + \frac{R}{r}\right).
$$

$\alpha = 2\pi a(r_1 + r_2)C\Delta x^2/\Delta t$,

$\beta_i = 2\pi a(r_1 + r_2)\Delta x^2[g_{Na}(V_i) + g_{k_1}(V_i) + g_{k_2}(V_i)]$,

$\gamma_i = 2\pi a(r_1 + r_2)\Delta x^2[g_{Na}(V_i)V_{Na} + (g_{k_1}(V_i) + g_{k_2}(V_i))V_k]$,

$$i = 1, \cdots, N - 1, N + 2, \cdots, N + M - 1,$$

where the conductances are shown to be functions of x and t through V, as defined by equations 10–12.

The unknowns $V(x_0, t + \Delta t)$ and $V(x_{N+M}, t + \Delta t)$ must be provided by the appropriate choice of boundary conditions. It is noted that β_i and γ_i contain n, m, and h evaluated at $t + \Delta t$. Each of the latter can be written in the form of equa-

tion 13 where the α_y and β_y are rate constants (different from α and β_i in equation 24). The quantity $g(V(x, t))$ indicates that the derivative depends on $V(x, t)$. Therefore, $y(x, t + \Delta t)$ can be approximated by

$$y(x, t + \Delta t) = g(V(x, t))\Delta t + y(x, t). \tag{25}$$

The quantity $y(x, 0)$ can be found by assuming that $\partial y/\partial t$ at $t = 0$ is zero and calculating from equation 13

$$y(x, 0) = \frac{\alpha_y}{\alpha_y + \beta_y},$$

where α_y and β_y are evaluated at $V(x, 0)$. The assumption of zero initial derivative is verified by the results; it will be seen that n, m, and h change slowly during the initial phases of depolarization when the membrane is essentially at rest.

The procedure for obtaining $V(x, t + \Delta t)$ can be summarized as follows.

(a) At $(t + \Delta t)$, $V(x, t)$ and $y(x, t)(y = m, n, \text{ or } h)$ have been determined. Initial condition $V(x, 0)$ given.
(b) Find $y(x, t + \Delta t)$ from equation 25 for n, m, and h.
(c) Calculate β_i and γ_i and substitute them into equation 24.
(d) Specify the boundary conditions at $t + \Delta t$.
(e) Solve the matrix equation 24.

Specification of $V(x, 0)$, $V(x_0, \Delta t)$ and $V(x_{N+M}, \Delta t)$ is needed to start the solution For $V(x, 0)$ we could choose the resting value of transmembrane voltage, V_r. However, one would then need a stimulus of some sort to excite the cell. This would appear as an additional term in equation 9. This initial condition, however, is somewhat inconvenient since the solution would include undesirable "starting-up dynamics." Since the primary puraose of the model is to study the effect of the gap parameters (i.e. the solution near $x = L_1$), it is desirable that the action potential approach that end with a constant velocity. Then, any changes in the waveform can be attributed to the gap effects only. Therefore, it is assumed that instead of the active cell being of length L_1, it is actually semi-infinite in length, terminating at $x = L_1$. The excitation starts at essentially $x = -\infty$ and proceeds to the right. It then approaches $x = 0$ with a constant velocity. Time, $t = 0$, is chosen to be that instant when the peak of the action potential is just to the left of $x = 0$. If this is the case, an electrotonic spread of potential is assumed to be exhibited in the region $x \geq 0$.

The boundary condition for $V(x_0, t + \Delta t)$ is chosen to be that potential which would be found if propagation from the left proceeds past the point at constant velocity; that is $V(x_0, t)$ is a normal action potential. Here it is assumed that the gap is far enough away so as not to affect this simplification; this approximation can be checked by an examination of the resulting solution.

At the end $x = L_1 + L_2$, a terminal condition must be specified. Since the fiber ends abruptly at this point (assuming only two cells), the longitudinal current I_1 and, therefore, $\partial V(x, t + \Delta t)/\partial x$ could, for example, be made zero. In difference form this condition reduces to

$$V(x_{N+M}, t + \Delta t) = V(x_{N+M-1}, t + \Delta t).$$

This boundary condition serves to change the $(N + M - 1, N + M - 1)^{st}$ element of the matrix in equation 24 to $-1 + \alpha + \beta_{N+M-1})$ and the $(N + M - 1)^{st}$ element of the input vector to $V(x_{N+M-1}, t) + \gamma_{N+M-1}$.

RESULTS

Equation 24 was solved for the two-cell interaction problem as outlined in the previous section. Constants for the cardiac cell were taken from various sources, primarily from Noble (9) to be:

a, radius of cell: 8 μ

g_{Na}, maximum Na$^+$ conductance: 0.4 mho/cm

g_{K_2}, maximum outward K^+ conductance: 1.2 mho/cm

C, membrane capacitance: 12 μF/cm

ρ, specific internal resistivity: 100 Ω-cm

r_1, internal specific resistance: $\rho/\pi a^2$ Ω/cm

r_2, external specific resistance, negligible compared to r_1

V_{Na}, Na$^+$ equilibrium potential: 40 mv

V_K, K^+ equilibrium potential: -100 mv

V_r, resting potential: -90 mv

L_1, L_2, length of cells: 0.1 cm

M, N, number of increments: 40

Δt, time increment: 0.2 msec

The length of the cell was taken to be about 10 times as large as a normal cardiac cell of approximate length 100 μ. This is because the spatial extent of the cardiac action potential encompasses many cell lengths (11) and it is desirable that L_1 be large enough so that one complete action potential be generated within the endpoints. The effect of the gap parameters is of primary interest. This, along with the fact that only depolarization can be simulated due to the large latency of the plateau, dictated the choice of L_1.

The initial condition $V(x, 0)$ and the boundary condition $V(0, t + \Delta t)$ were discussed previously. The only remaining parameters in equation 24 that need specification are the resistance variables R and r. The choice of both is arbitrary and the problem is solved for many different sets of R and r.

Figs. 7 and 8 show the results of the cardiac cell interaction simulations. Several sets of values for R and r, the parameters of the gap region, were used in the model

in order to determine those sets which permitted transmission. Figs. 7 A and 7 B are the spatial and temporal results of one particular set which easily passed an action potential, namely $R = r = 5 \times 10^5 \, \Omega$. The vertical bar at $x = 0.1$ denotes the gap region. (The gap width is not to scale; it is actually much narrower than is indicated.) It is seen that there is relatively little distortion in the spatial curves due to the gap except when the peak is centered near the gap. The temporal variation at $x = 0.105$, which is the first node of the inactive cell, is somewhat distorted but does eventually reach full value. The gap also produces a latency in the waveform as it decreases the velocity of propagation through the gap. This is indicated by the
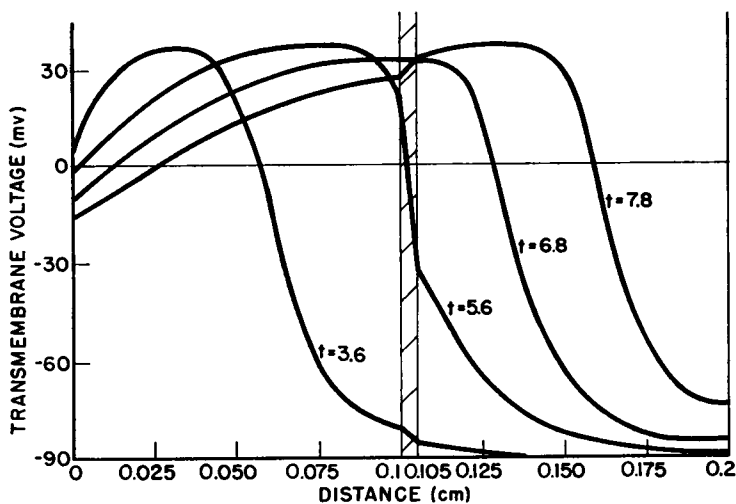
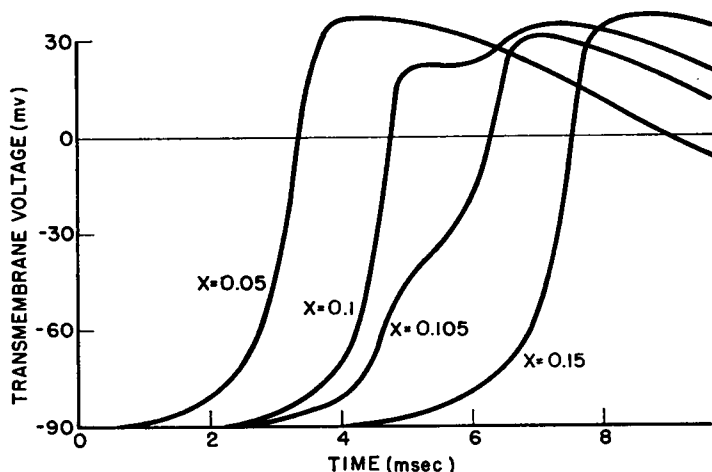FIGURE 7 A Transmembrane voltage vs. distance. $R = r = 5 \times 10^5 \, \Omega$.

FIGURE 7 B Transmembrane voltage vs. time. $R = r = 5 \times 10^5 \, \Omega$. Time ($t$) in msec.

separation of the peaks at $x = 0.1$ and $x = 0.105$. Finally, the point $x = 0.15$ undergoes a normal action potential indicating full recovery at the midpoint of the second fiber.

Figs. 8 A and 8 B show the temporal variations at $x = 0.1$ and $x = 0.105$, respectively, for a range of values for r. The action potentials at $x = 0.105$ all eventually go positive if the second fiber fires at all. Of course, there are certain values of r for which there is no transmission. A firing threshold was found for the second cardiac fiber to be in the range 16–20 mv above resting.

Fig. 9 summarizes the interaction simulation and indicates the results of examining several sets of R and r. Each cross or point represents an experiment, as a
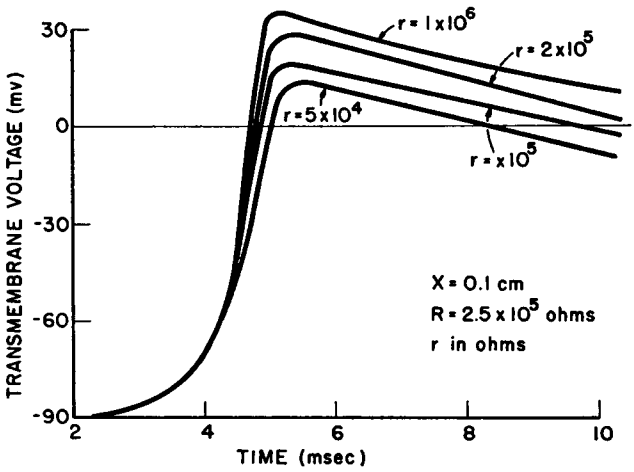

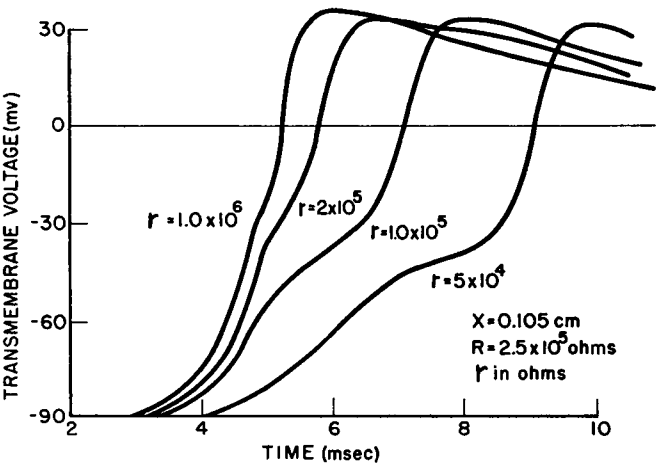FIGURE 8 A   Transmembrane voltage vs. time. $x = 0.1$ cm. $R = 2.5 \times 10^5 \, \Omega$. r in Ω.

FIGURE 8 B   Transmembrane voltage vs. time. $x = 0.105$. $R = 2.5 \times 10^5 \, \Omega$. r in Ω.

+ DENOTES FIRING
O DENOTES NONFIRING

R = r

r
(ohms)

10^6

10^5

10^4

ACTIVE BOUNDARY

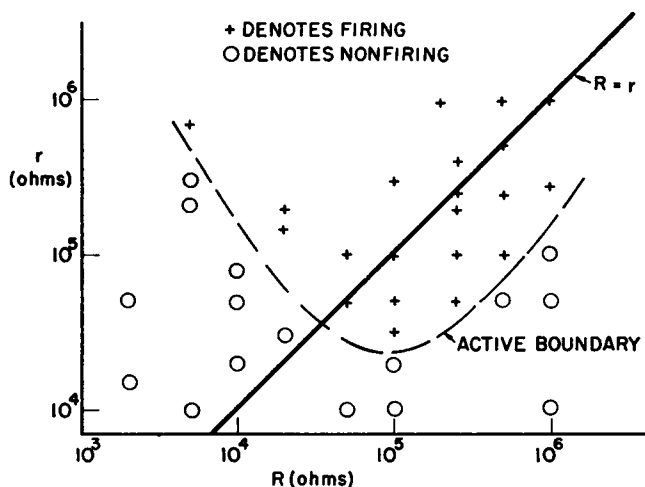10^3 10^4 10^5 10^6

R (ohms)

FIGURE 9   Summary of firing results. + denotes firing. 0 denotes nonfiring.

result of which the inactive cell either fires or doesn't fire, respectively. For reference, the line $R = r$ is included in the drawing. It is seen that the points producing firing are clustered in a "region of firing" which is delineated from those not producing excitation by a line labeled "active boundary." The farther within the region of firing and away from the boundary, the more efficient is the transmission in terms of the time delay produced by the influence of the gap upon propagation velocity.

It is apparent that certain values of r may be less than R and still provide for transmission. In general, however, for the range of R that is expected ($<10^5$), r should be at least as large as R. Referring back to Table I, it is seen that the condition $r \geq R$ fixes the maximum allowable value of R_d, the specific intercalated disc resistance, to be approximately 4 Ω-cm^2 at $\delta = r_o/10^3$. This corresponds quite well with experimental determinations of R_d (reference 5).

DISCUSSION AND CONCLUSIONS

This analysis confirms the low resistance requirement which must be met if the intercalated disc is to permit electrical transmission in the heart. Furthermore, the model permits a consideration of the effect of intercalated disc and gap parametric values on the properties of the resultant action potential propagation such as velocity, current flow, waveform, and magnitude. The model demonstrates a particular usefulness in a problem where direct physical measurements are very difficult. It should, however, be noted that the validity of the results depends on the chosen geometry, the Noble-modified Hodgkin-Huxley dynamic equations, and several additional, stated assumptions.

One important simplification is the assumed inexcitability of the disc resistance. Consequences of an excitable disc resistance upon interaction have not been in-

vestigated. However, since excitable membrane shows a large decrease in resistance during activation, and since the model requires low values of R_d, the assumption is probably not a critical one. Had the requirement on R_d come out large, then the results could strongly depend on the specific value of R_d.

The interaction results of Fig. 9 suggest that the gap model may not be completely satisfactory. The shape of the "active boundary" for R less than 10^5 is not expected, intuitively, and indicates that a more sophisticated model of the gap is needed (perhaps one including an excitable disc resistance).

Other electrophysiological problems can be studied using models of this type. For instance, this model can be extended to determine velocity changes in a tapering nerve fiber simply by making the radius a function of distance. This study would be of interest since nerve fibers decrease in diameter as they approach synapses, the junction sites of nerve fibers. Also, it could be modified in order to examine lateral interaction which would occur where fibers are densely packed as in a nerve bundle.

REFERENCES

1. WOODBURY, J. W., and W. E. CRILL. 1961. *In* Nervous Inhibition. E. Florey, editor. Pergamon Press Ltd., Oxford.
2. NOBLE, D. 1965. *J. Cell. Comp. Physiol.* **66**:127.
3. WOODBURY, J. W., and A. M. GORDON. 1966. *J. Cell. Comp. Physiol.* **66**:35.
4. BARR, L., W. BERGER, and M. M. DEWEY. 1968. *J. Gen. Physiol.* **51**:347.
5. WEIDMANN, S. 1966. *J. Physiol. (London).* **187**:323.
6. WOODBURY, J. W., and W. E. CRILL. 1970. *Biophys. J.* **10**:1076.
7. HODGKIN, A., and A. HUXLEY. 1952. *J. Physiol. (London).* **117**:500.
8. HODGKIN, A., A. HUXLEY, and B. KATZ. 1949. *Arch. Sci. Physiol.* **3**:129.
9. NOBLE, D. 1966. *Physiol. Rev.* **46**:1.
10. CRANK, J., and P. NICHOLSON. 1947. *Proc. Cambridge Phil. Soc.* **43**:50.
11. VANDERARK, D., and E. REYNOLDS. 1967. *Circulation.* **35**(2):255.